EXPERIMENTAL AND NUMERICAL STUDIES OF TWO PHASE FLOW REGIMES AROUND A CIRCULAR CYLINDERTHROUGH AN ENLARGING CHANNEL

Laith Jaafer Habeeb
Mechanical Engineering Dept.,University of Technology, Baghdad – Iraq
(e-mail: laithjaafer@yahoo.com , or, dr.laith_jaafer@uotechnology.edu.iq)

ABSTRACT

Experimental and numerical studiesare investigated to study the two-phase flow phenomena around a circular cylinder in a rectangular enlarging channel which has the dimensions (10 × 3 × 70 cm) enlarged from assembly circular tube of the two phases. Experiments are carried out inthe channel with air-water flow with different air and water flow rates. These experiments are aimed to visualize the two phase flow phenomena as well as to study the effect of pressure difference through the channel with the cylinder. All sets of the experimental data in this study are obtained by using a pressure transducer and visualized by a video camera for different water discharges (20, 25, 35 and 45 l/min) and different air discharges (10, 20, 30 and 40 l/min). Whilethe numerical simulation is conducted by using commercial Fluent CFD software to investigate the steady and unsteadyturbulent two dimensional flows for different air and water velocities with smooth enlargement. The results showed that the when air discharge increases, high turbulence is appear which generate more bubbles and waves.

Key words: air-water two-phase flow, smooth enlargement, rectangular channel, steady and unsteady turbulent flow.

دراسة عملية ومحاكاة نظرية لجريان ثنائي الطور حول اسطوانة دائرية خلال مجرى مستعرض

الخلاصة :-

تحقق في هذا البحث دراسة عملية ومحاكاة نظرية لدراسة ظاهرة الجريان ثنائي الطور حول اسطوانة دائرية في مجرى مستطيل مستعرض (10*3*70 سم) من انبوب دائري متداخل للطورين. تم اجراء التجارب في المجرى بوجود جريان هواء- ماء وبمديات مختلفة لجريانات الهواء والماء. ان هذه التجارب تهدف الى تصوير ظاهرة الجريان ثنائي الطور وكذلك لدراسة تأثير فرق الضغط خلال المجرى مع الاسطوانة. كما ان كل النتائج المستحصلة من التجارب في هذه الدراسة قد تمت بإستخدام متحسس ضغط وان التصوير الفيديوي قد تم بإستخدام كاميرا فيديو حديثة وذلك لجريانات مختلفة للماء (20 و 25 و 35 و 45 لتر/ دقيقة) ولجريانات مختلفة للهواء (10 و 20 و 30 و 40 لتر/ دقيقة) . بينما

المحاكاة النظرية قد تمت بإستخدام برنامج Fluent لإستعراض الجريان المضطرب ثنائي البعد للحالة المستقرة وغير المستقرة ولسرع مختلفة للهواء والماء مع توسع سلس.اظهرت النتائج انه في حالة زيادة تدفق الهواء فسيظهر اضطراب عالي ويولد فقاعات وامواج اكثر.

كلمات مفتاحية: جريان ثنائي الطورهواء- ماء ،توسع سلس ، مجرى مستطيل ، جريان مضطرب للحالة المستقرة وغير المستقرة.

NOMENCLATURE :-

$\vec{F}$	Body force	(N)
$\vec{g}$	Gravityacceleration	(m/s^2)
n	Number of phases	(-)
Q	Discharge	(l/min)
t	Time	(sec)

Greek Symbols

α_k	Volume fraction of phase k	(-)
ρ_m	Mixture density	(kg/m^3)
$\vec{v}_m$	Mass-averaged velocity	(-)
$\vec{v}_{dr,k}$	Drift velocity for secondary phase k (velocity of an algebraic slip component relative to the mixture)	(-)
μ_m	Viscosity of the mixture	(N/m^2.s)

Subscripts

a	Air
k	Secondary phase
m	Mixture
w	Water

1- INTRODUCTION :-

From a practical engineering point of view one of the major design difficulties in dealing with two-phase flow is that the mass, momentum, and energy transfer rates and processes can be quite sensitive to the geometric distribution or topology of the components within the flow. Usually the flow patterns are recognized by visual inspection, though other means suchas analysis of the spectral content of the unsteady pressures or the fluctuations in the volume fraction have been devised for those circumstances in which visual information is difficult to obtain.The flow patterns of gas-liquid two-phase flow could be bubble flow, slug flow, plug flow, stratified flow, wavy flow and disperse flow. There are still many challenges associated with a fundamental understanding of flow patterns in multiphase flow and considerable research is necessary before reliable design tools become available.Gas-liquid flow was extensively used in industrial systems such as power generation units, cooling and heating systems (i.e. heat exchangers and manifolds), safety valves, etc.These systems normally have complex geometries composed by singularities like expansion, contraction, bends and orifices.

Thus two-phase flow characteristics through these singularities should be identified in order to be used in designing of the systemBrennen 2005.
HAORAN 1993was concerned with phase distributions in low-quality dispersed two-phase flows past obstacles and comprised a theoretical part of a more general nature and an experimental part highlighted bubbly flows past obstacles in vertical tubes. The theoretical study aimed at improving modeling algorithms for predicting phase distributions around obstacles as well as at gaining a better understanding of the interaction between the dispersed phase and its carrier fluid as a dispersed two-phase flow passes an obstacle. The single-phase (or continuous-phase) carrier fluid flow past an obstacle was the starting point for the modeling of the interaction process between the two phases and was formulated based on empirical data. In the experimental part, two measuring systems were applied to take measurements of phase distributions of bubbly flows past obstacles over a wide range of experimental conditions, under both the atmospheric pressure and high pressures. Parallel to the corresponding theoretical studies, effects of the main system parameters on phase distributions of the bubbly flows were investigated.EAMES et al.2004 derived a general estimates for mean velocities through and around groups or arrays offixed and moving bodies, in unbounded and bounded domains, which lie within afinite perimeter. Robust kinematic flow concepts were introduced, namely the Eulerian spatial mean velocity in thefluid volume between the bodies, the Eulerian flow outside the group and the Lagrangian mean velocity of material surfaces or fluid particles as they pass through the group of bodies. The Eulerian mean velocity is related to the momentum in the fluid domain, and was mainly influenced by fast moving regions of the flow. When the bodies were well-separated, the interstitial Eulerian and Lagrangian mean velocities were defined and calculated in terms of the far-field contributions from the velocity or displacement field within the group of bodies. In unbounded flow past well-separated bodies situated within a rectangular perimeter, the difference between the Eulerian and Lagrangian mean velocity is negligible.
Zhang et al. 2008 presented the steady computational fluid dynamic (CFD) results of cavitation in liquid nitrogen flow through hydrofoils and ogives with so-called ‘‘full cavitation model”. The model was reexamined to assess the performance prediction from the standpoint of cryogenic fluids with the assumption of thermal equilibrium between vapor phase and liquid phase. The full cavitation model with the default coefficients was applicable for cavitation prediction in liquid nitrogen, taking into account of the thermodynamic effects. Krepperet al. 2009concerned with the model of a polydispersed bubble population in the frame of an ensemble averaged two-phase flow formulation. The ability of the moment density approach to represent bubble population size distribution within a multidimensional CFD code based on the two-fluid model was studied. Two different methods describing the polydispersion were presented: (i) a moment density method, developed at IRSN, to model the bubble size distribution function and (ii) a population balance method considering several different velocity fields of the gaseous phase. The first method was implemented in the Neptune_CFD code, whereas the second method was implemented in the CFD code ANSYS/CFX. Both methods consider coalescence and breakup phenomena and momentum interphase transfers related to drag and lift forces. Air-water bubbly flows in a vertical pipe with obstacle of the TOPFLOW experiments series used as simulations test cases. The numerical results, obtained with Neptune_CFD and with ANSYS/CFX, allow attesting the validity of the approaches.Hao Zhou et al. 2011investigated the vortex structures and particle dispersions inflows around a circular cylinder by lattice Boltzmann method (LBM), with non-equilibrium extrapolation method (NEM) dealing with the computational boundaries. The particles were traced in the Lagrangian framework. The effect of the Reynolds number (Re = 40–100) on the evolution of the vortex structures was investigated. Good agreements of the drag coefficient, lift coefficient and the Strouhal number were achieved with previous studies. It was found that both the

Reynolds number and the Stokes number produce significant influences on the particle distribution. The small particles (St = 0.01) follow the motion of the fluid very well and can disperse into the core regions of the vortex structures. The particles at intermediate Stokes numbers (St = 0.1 and 1) concentrate on the boundaries of the vortices, and the large particles (St = 10) also assemble in the outer regions of the vortices under the influence of the vortex structures.Bon 2011 studied two different air-water interfacial flows including plunging wave breaking and flow past a vertical surface-piercing circular cylinderusing complementary CFD Ship-Iowa version 6 including Cartesian grid solver and orthogonal curvilinear grid solver.The simulations showed differences and similarities with other experimental and computational studies for wave breaking in deep water and sloping beaches. The flow features near the air-water interface showed significant changes with different Reynolds numbers from sub-critical to critical regime. It was shown that the interface made the separation point more delayed for all regimes of Re. Talimi et al. 2012 reviewed numerical studies on the hydrodynamic and heat transfer characteristics of two-phase flows in small tubes and channels. The review was then categorized into two groups of studies: circular and non-circular channels. Different aspects such as slug formation, slug shape, flow pattern, pressure drop and heat transfer were of interest. Gaps in research were found in applications of non-circular ducts, pressure drop and heat transfer in meandering microtubes and microchannels for both gas–liquid and liquid–liquid two-phase flows.

Emrah 2011 studied characteristics of adiabatic air-water flow through a horizontal channel having smooth expansion (enlarging), which was obtained by inspiring from one of the singularities existing in safety valves, were investigated numerically. Numerical simulations are performed via commercial software, GAMBIT (v. 2.3.16) and FLUENT(v. 6.3.26), for the flow upstream, through and downstream the singularity. Eulerian Model was employed for the analysis. Internal diameter of the channel enlarges from 32 mm to 40 mm. Flow rate for water was constant at 3 l/s while that for air was taken as 50 and 61 l/min.

From the previous review it is denoted that the recent researches in the two phase flow with the enlargement and existence of a circular cylinder are very limited. So, my concern in this study is to study the effects of wide range of air/water discharge in the steady and unsteady cases on the flow behavior with the enlargement from the circular tube of the water phases which contains the air phase tube, to the rectangular duct with the existence of a circular cylinder.

2-THE PHYSICAL MODEL AND EXPERIMENTAL APPARATUS

Fig.1 shows a schematic and photograph of the experimental Apparatus and measurements system.The rigis consists of, as shown in Fig. 2:

1- Main water tank of capacity (1 m^3), valves and piping system (1.25 in).
2- Water pumpconnected with flow meter its type is Hitachi Ltd.(ov) and it has specification quantity (0.08 m^3/min) and head (8 m).
3- Adjustable volume flow rate of range (10-80 l/min) is used to control the liquid (water) volume flow rates that enter test section.
4- Aircompressor[Recomendamos Aceite/Worthingtontype] and it has a specification capacity of (0.5 m^3
5- Pressuretransducer sensors which are used to record the pressure field with a range of (0-1 bar) and these pressure transducer sensors are located in honeycombs at the entrance and at the end of the test section. The pressure sensors with a distance of (80 cm) between each other are measuring with an accuracy of (0.1%).

6- Rotameter was used to control the gas (air) volume flow rates that enter the test section. It has a volume flow rate range of (6-50) l/min.
7- The two enlargement connecting parts are made of steel and manufactured with smooth slope. The first on is used to connect the test section with the outside water pipe in the entrance side while the second oneis used to connect the test section with the outside mixture pipe in the exit side. The inside air pipe,in the entrance side, is holed and contained inside the water pipe by asteel flange.
8- The test section is consisting of rectangular channel and a circular cylinder. The rectangular cross sectional area is (10 cm ×3cm) and haslength of (70 cm) which is used to show the behavior of the two phase flow around the circular cylinder and to measure the pressure difference and records this behavior.The circular cylinder is mounted and fixed by screw and nut on a blind panel on the bottom of the rectangular channel.The three large Perspex windows of the channel (two lateral sides with lighting and the top side) allowing optical access through the test section. The circular cylinder used is made of stainless steel and its dimensions are (3 cm) diameter and (3 cm) length which is coated with a very thin layer of black paint and its center located at (11.5 cm) from the entrance of the test section.
9- Interfacesystem which is connected with a personal computer so that the measured pressure across the test section is displayed directly on the computer screen by using a suitable program. The interface system consists of two parts which are the data logger and the transformer which contains in a plastic box. The data logger has a three connections two of them are connected to the outside of the box (one connected to the sensors and the other connected to the personal computer), the third connection is connected to the transformer, which is work to receive the signals as a voltage from the sensors and transmit it into the transformer and then re-received these signals after converting it to ampere signals in the transformer.
10- A Sony digital video camera recorder of DCR-SR68E model of capacity 80 GB with lens of Carl Zeiss Vario-Tessar of 60 x optical, 2000 x digital is used to visualize the flow structure.The visualized data are analyzed by using a AVS video convertor software version 8.1. A typical sequence snapshots recorded by the camera using a recording rate of 30 f/s.

For more accuracy in the experimental work, calibrations of the rig measuring devices are done. The flows of both gas and liquid are regulated respectively by the combination of valves and by-passages before they are measured by gas phase flow meter and liquid phase flow meter. The gas phase and the liquid phase are mixed in the enlargement connection part before they enter the test section. When the two-phase mixture flows out of the test section, the liquid phase and the gas phase are separated in liquid storage tank.Experiments were carried out to show the effect of different operation conditions on pressure difference across the test section and to visualizethe flow around the circular cylinder. These conditions are water discharges and air discharges. The selected experimental values are presented in **Table 1**.

The experimental procedures are:

1- Turn on the water pump at the first value (20 l/min).
2- Turn on the air compressor at the first value (10 l/min).

) and maximum pressure of (16 bars), valves, piping system (0.5 in) and gages.

3- Record the pressure drop through the test section and photographthe motion of the two-phase flow by the digital camera.
4- Repeatthe above steps by changing the water discharge according to **Table 1**.
5- Repeat the above steps by changing the air discharge according to **Table1**.

These give sixteen (16) cases for volume fraction (Air/Water ratios).

2- NUMERICAL MODELING

In this study, the computational fluid dynamics (CFD) software have been applied for the numerical simulation for adiabatic gas-liquid flow characteristics through a horizontal channel contain a circular cylinder with smooth expansion from the liquid pipein steady, unsteady and 2D cases. In order to compare numerical results with experimental ones, air-water couple has been selected as the representative of the gas-liquid two-phase flow. Construction of the numerical domain and the analysis are performed via GAMBIT and FLUENT (ANSYS 13.0) CFD codes, respectively. Two-phase flow variables such as void fraction and flow velocity for liquid (water) and gas (air) at the inlet condition, and the geometrical values of the system (i.e. channel length, width and height, pipes and inlet enlargement connecting part dimensions, and cylinder diameter) used in the analysis are selected as the same variables as the experimental part. Atmospheric conditions are valid for the experimental facility. Total test rig length in the experiments, thus in the numerical domain, is (100cm) including (70cm) for the test section containing cylinder, and (30cm) for the inlet enlargement part. Water pipe diameteris (3.175cm) and air pipe diameter is (1.27 cm) as shown in Fig. 3.

The 2Dphysical model is established using a model of flow focusing channel in CFD. The enlargement connecting part length consists of: (0.05 m) circular pipe, (0.15 m) diverge-link to change the shapefrom circular to rectangular and (0.1 m) rectangular duct. Air and water are selected to be working fluids and their fluid properties are in **Table2**.

The model geometry structure was meshed by the preprocessor software of GAMBIT with the Quad/Pave grids. After meshing, the model contained 14978 grid nodes and 14522 cells for 2D -as demonstrated in Fig. 4 -before importing into the processor Fluent for calculation. This refinement grid provided a precise solution to capture the complex flow field around the cylinder and mixing region in the enlargement connecting part. The boundary conditions are the velocity inlet to the air and water feeding (Table 3) and the pressure outlet to the model outlet. A full geometry is considered because of the asymmetry behavior of the mixture that appeared in the movies when photographing the experiences as will be shown later. In Fluent, the Mixture model was adopted to simulate the flow.The mixture model is a simplified Eulerian approach for modeling *n*-phase flows**(FLUENT 2006)**. Because the flow rates of the air and water in the channel arehigh, the turbulentmodel (k-ε Standard Wall Function) has been selected for calculation. The other options in Fluent are selected: SIMPLE (Semi-Implicit Method for Pressure-Linked Equations) scheme for the pressure-velocity coupling, PRESTO (pressure staggering option) scheme for the pressure interpolation, Green-Gauss Cell Based option for gradients, First-order Up-wind Differencing scheme for the momentum equation, the schiller-naumann scheme for the dragcoefficient, manninen-et-al for the slip velocity and other selections are described in **Table 4**. The time step (for unsteady case),maximum number of iteration and relaxation factorshave been selected with proper values to enable convergence for solution which is equal to (0.001) for all parameters.

The hydrodynamics of two-phase flow can be described by the equations for the conservation of mass and momentum, together with an additional advection equation to determine the gas-liquid interface. The two-phase flow is assumed to be incompressible since the pressure drop along the axis orientation is small. For the incompressible working fluids, the governing equations of the Mixture formulations on multiphase flows are as following (**ANSYS 13)**:

The continuity equation for the mixture is:

$$\frac{\partial}{\partial t}(\rho_m) + \nabla \cdot (\rho_m \vec{v}_m) = 0 \qquad (1)$$

Where $\vec{v}_m$is the mass-averaged velocity:

$$\vec{v}_m = \frac{\sum_{k=1}^{n} \alpha_k \rho_k \vec{v}_k}{\rho_m} \qquad (2)$$

and ρ_m is the mixture density:

$$\rho_m = \sum_{k=1}^{n} \alpha_k \rho_k \qquad (3)$$

$\alpha_k$is the volume fraction of phase k .

The momentum equation for the mixture can be obtained by summing the individual momentum equations for all phases. It can be expressed as:

$$\frac{\partial}{\partial t}(\rho_m \vec{v}_m) + \nabla \cdot (\rho_m \vec{v}_m \vec{v}_m) = -\nabla p + \nabla \cdot [\mu_m (\nabla \vec{v}_m + \nabla \vec{v}_m^T)] + \rho_m \vec{g} + \vec{F} + \nabla \cdot \left(\sum_{k=1}^{n} \alpha_k \rho_k \vec{v}_{dr,k} \vec{v}\right) \qquad (4)$$

where n is the number of phases$\vec{F}$, is a body force, and μ_m is the viscosity of the mixture:

$$\mu_m = \sum_{k=1}^{n} \alpha_k \mu_k \qquad (5)$$

$\vec{v}_{dr,k}$ is the drift velocity for secondary phase k :

$$\vec{v}_{dr,k} = \vec{v}_k - \vec{v}_m \qquad (6)$$

In FLUENT application, boundary conditions like “velocity inlet” is taken as the inlet condition for water and air while “interior” and “outflow” are employed as the water-air mixture. Air is injected to the water via an air pipe in the experiments, therefore, the gas flow through the air pipe and the mixture occurred outlet of it are modeled in 3D (Fig.3). According to the simulation, air with known mass flow rate flows through air pipe and then disperses into the water at the exit of the pipe. At air flow rates (thus volumetric void fraction), phase inlet velocity and void fraction profiles obtained at the air and water pipes outlet are extracted from the experimentalcalculations in order to be introduced as the inlet condition for the flow analysis regarding the numerical 2D domain.In the present study bubble diameter is equal to (1 cm). Assuming the bubbles are in spherical shape and neglecting the coalescence between them along the channel.

3- EXPERIMENTAL RESULTS

The experimental results are representedasvisualizations of a circular cylinder in gas-liquid flow through channel for different water discharges (20, 25, 35 and 45l/min) and different air discharge (10, 20, 30 and 40l/min) as photographs and pressure graphs.

4-1 Effect of Water Discharge

Fig.s (5-a, b, c & d) showphotographs for the two phase flow behavior around the cylinder for air discharge (Q_a=10 l/min) and water discharges(Q_w=20, 25, 35 and 45l/min) from top to bottom respectively.It shows that the number (amount) of bubble is few and has small size at low water discharge.Photographs (5-a&b) describe the flow behavior andit appears that itis near to slug or plug region. This is due to the low velocity of water at low water discharge.

Also when increase the air discharge the size and number of bubbles increases and the bubble cavities develops to cloud cavitations especially at highair discharge. This is due to the high velocity of water at high water discharge which leads to more turbulence in the flow and the flow becomes bubbly as shown in photographs (5-c&d). Fig.s (6-a, b, c & d) showphotographs for the two phase flow behavior for air discharge (Q_a=20 l/min) and water discharges (Q_w=20, 25, 35 and 45l/min) from top to bottom respectively.It is clear thatthe flow becomes unstable and unsymmetrical around the circular cylinder and the number and size of bubble become higher compared with theprevious case.It appearsthat the vortices behind and beside the cylinderbecomes more strong compared with theprevious case.Fig. 7represents photographs for the flow behavior around the cylinder for air discharge (Q_a=30 l/min) and the same water discharges.While Fig. 8representsphotographs for air discharge (Q_a=40 l/min) and the same water discharges. More unsteady behavior is noticed and the flow oscillates between bubble and disperse regions. When water discharge increases with increase air discharge, flow becomes unsteady, vortices developed around the circular cylinder surface and most bubbles transformed to cloudyflow, then a disperse regionand strong vortex shedding is observed.

Also when air discharge increases, high turbulence appears which generate more bubbles and waves.This is due to the important effectof the cylinder existence in rectangular channel which effect on pressure difference across the inlet and outlet the channel.

4-2Effect of Time Evolution of Pressure

Fig. 9 represents the effect of time evolution of pressure obtained by experiments for water discharge Q_w=20 l/min and air discharge Q_a=10 l/min at inlet and outlet of the rectangular channel across the circular cylinder**.** The pressure sensor at the inlet -after honeycombs- and outlet of the test section are record pressuresthat fluctuating as a function of time due to two-phase effect.

4-3Effect of Pressure Difference

Fig. 10 represents the mean pressure difference with water discharge for different values of air discharge**.**While Fig. 11 shows the mean pressure difference with air discharge for different values of water discharge**.**When air or water discharge increases, the mean pressure difference increases. This is due to the increase of air or water discharge resulting in velocityincreases.It is already noticed that the mean pressure difference has a significant influence on two-phase flow behavior. Therefore, it is expected that the flow instability will also depend upon the pressure difference.

5-NUMERICAL RESULTS

The numerical results are represented as contours and vectors for the same air-water discharges cases in the experimental part (**Table 3**). As mentioned above, the 2D inlet (line) air or water velocities are calculated from the 3D experimental inlet (surface) area from the air or water discharge.

5-1 Steady State

Fig.s (12-a, b, c, d, f and g) depictvolume fraction (water) contours for selected cases (case1, 3, 5, 6, 10, 11 and 12respectively).The differences between the experimental snapshots and numerical Fig.s are due to two reasons; the first is the differences in the overall flow rates of air and water for the same inlet velocities from the inlet regions (small lines in 2D numerical cases and big square and annulus areas in 3D experimental cases), and the second reason is that the snapshots are taken roughly from the experimental movies for each case and may be for another snapshot from the same case movie, the differences will be less. From Fig. 12it is appear that a slug to disperse regionsflow pattern is achieved.The flow rates of air and water have a large range.Fig.s (12-a and b) show the increase in water phase and with the decrease of the gas flow rate, the volume fraction of the gas decreased and the volume fraction of the water increased simultaneously. Fig.s (12-c and d) present the increase of air and water cases respectively with the respect of previous. According to the figures, stratified water-air mixture enters the singularity section and begins to decelerate due to the smoothly enlarging cross-section. While Fig.s (12-e, f and g) represent how the volume fraction affected the flow behavior. A uniform dispersed two-phase flow, in which the dispersed phase (either air bubbles or water droplets) moves with their carrier fluid (water or air), approaches to a circular obstacle. Due to strong changes of both magnitude and direction of local velocities of the fluid flow (i.e. local fluid velocity gradients) and density difference between the dispersed phase and the fluid, the local phase distribution pattern changes markedly around the obstacle.

Fig.s (13-a, b, c, d, f and g) showselected focused area of velocity vectors colored by volume fraction (water) for othercases (a- case2, b- 4, and c- 9respectively) and contours of turbulent viscosity (mixture) in (kg/m.s) for another different cases (d- case7, e- 14and f- 16 respectively).Fig.s (13-a, b and c)represent the calculated local velocities in the flow field around the cylinderwith the potentialflow regionat different air/water velocity ratios.Strong air flows are induced and a strong vortex is created as a result of the entered air and small vortices are also produced.A recirculation zone in the wake, flow separation at the edge of the obstacle and a wavy motion are noticed. Fig.s (13-d, e and f) depictturbulent viscosity of the mixture (eq.(5)), it is appear that maximumturbulent viscosity and high turbulence regions depends on the volume fraction ratio. Also, when air velocity increases, separation area is detected after the cylinder.

5-2 Unsteady State

Fig.s (14-a, b, c, d, e and f) represent volume fraction (water) contours development for randomly selected unsteady case8. It show how the volume fraction develops with time. As can be seen, there are two unsteady asymmetrical pattern recirculating zones behind the circular cylinderwhen the volume fraction increases or when the two-phase velocity(Reynolds number)increases.

Fig.s (15-a, b, c, d, e, f, g, h, i, j, k and l) represent center line (x=0.05 m) of the static and dynamic pressure distributions of the mixture along the test rig (1 m) for unsteady case8 at different time steps. It show how the pressures are fluctuating along the channel and the fluctuation is increases with time due to the effects of mixing, two-phase flow, circular cylinder existence and density difference.Region that the line does notpassing through it(i.e. empty at position (z) =0.115 m) is the circular cylinder area, as well as at the beginning (z = -0.3 to z=-0.28 cm)there is no mixing.

6-CONCLUSIONS

The study has focused on phase distributions in low quality dispersed two phase flows around obstacle. It consists of a theoretical part of a more general nature and an experimental part highlighting bubbly flows around a cylinder in horizontal channel. Concluding remarks are summarized below-

1- A novel approach for fluid dispensing with highconsistency and accuracy had been proposed based on the fluid dynamics of the gas-liquid two-phase flow.
2- When air discharge increases, high turbulence is appear which generate more bubbles and waves.
3- The pressure sensor at the inlet and outlet of the test section are record pressures that fluctuating as a function of time due to two-phase effect. Also, when air or water discharge increases, the mean pressure difference increases.

4- Due to strong changes of both magnitude and direction of local velocities of the fluid flow and density difference between the dispersed phase and the fluid, the local phase distribution pattern changes markedly around the obstacle.
5- Realistic bubble trajectories, with a number of bubble trajectories entering the wakeof a cylinder, are only obtained if the effect of liquid velocity fluctuations (or turbulencein the liquid) is simulated and some kind of sliding phenomenon for colliding bubbles istaken into account.
6- The effect of the existence of a circular cylinder is clear in dividing the two-phase flow, generate vortices and finally enhance mixing.
7- In this study, diameter of the bubbles is considered constant and coalescence between the bubbles is neglected. However, bubbles in the actual flow break down and unite as the flow develops along the channel and this gives a varying diameter distribution which causes lift and drag forces to be calculated locally. Therefore, a simulation considering the effects of differing bubble diameter and interfacial forces is suggested for better modeling of the flow investigated.

Table 1 Values of operation conditions used in experiments.

Water discharges (l/min) (Q_w)	20	25	35	45
Air discharges (l/min) (Q_a)	10	20	30	40

Table 2 Property parameters of the gas and liquid in CFD.

Fluid	Density (kg/m^3)	Viscosity (kg/m.s)	Surface Tension
Water	998.2	10.03×10^{-04}	0.072
Air	1.225	1.7894×10^{-05}	---

Table 3Air-water flow cases.

Case number	Air/water discharges (l/min)	Air/water velocities (m/sec)	Case number	Air/water discharge (l/min)	Air/water velocities (m/sec)
case1	10/20	1.32/0.50	case5	20/20	2.63/0.50
case2	10/25	1.32/0.63	case6	20/25	2.63/0.63
case3	10/35	1.32/0.87	case7	20/35	2.63/0.87
case4	10/45	1.32/1.12	case8	20/45	2.63/1.12
Case number	Air/water discharge (l/min)	Air/water velocities (m/sec)	Case number	Air/water discharge (l/min)	Air/water velocities (m/sec)
case9	30/20	3.95/0.50	case13	40/20	5.26/0.50
case10	30/25	3.95/0.63	case14	40/25	5.26/0.63
case11	30/35	3.95/0.87	case15	40/35	5.26/0.87
case12	30/45	3.95/1.12	case16	40/45	5.26/1.12

Table 4 Other mixture model selections for Fluent.

<table>
<tr><th>Solver type</th><th>k-ε Model</th><th>Solution Methods</th></tr>
<tr><td>Pressure-Based</td><td>Cmu=0.09, C1-Epsilon=1.44, C2-Epsilon=1.92</td><td>Volume Fraction and Turbulent Kinetic Energy (First-order Up-wind)</td></tr>
<tr><td colspan="3">Starting Solution Controls (Under-Relaxation Factors)</td></tr>
<tr><td colspan="3">Pressure=0.3, Momentum=0.7, Turbulent Kinetic Energy & Turbulent Dissipation Rate=0.8</td></tr>
<tr><td colspan="3">Specification Method for turbulence</td></tr>
<tr><td colspan="3">Intensity and Hydraulic Diameter (Turbulent Intensity=3% and Hydraulic Diameter=0.0127 m)</td></tr>
<tr><td colspan="3">Solution Initialization</td></tr>
<tr><td colspan="3">Turbulent Kinetic Energy (m^2/s^2)=0.0003375, Turbulent Dissipation Rate (m^2/s^3)= 0.0007620108 and air-bubble Volume Fraction=0</td></tr>
</table>

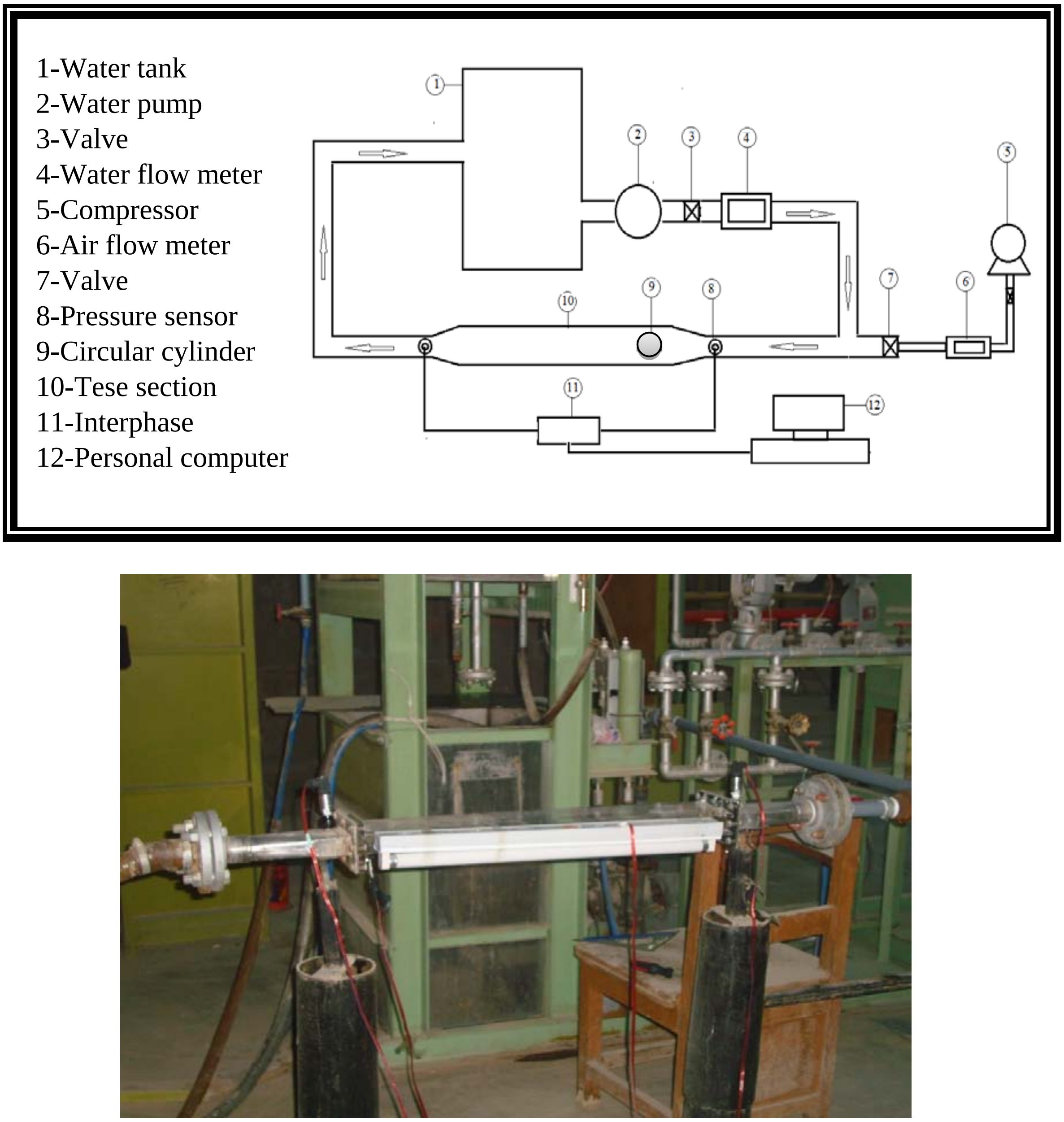

Figure 1 The experimental rig and measurementssystem (**Esam and Riyadh 2012)**.

(a) (b) (c)

Figure 2 (a) Water system, (b) Air flow meter, (c) Enlargement connecting part, flange, piping system and pressure transducer sensor(**Esam and Riyadh 2012)**.

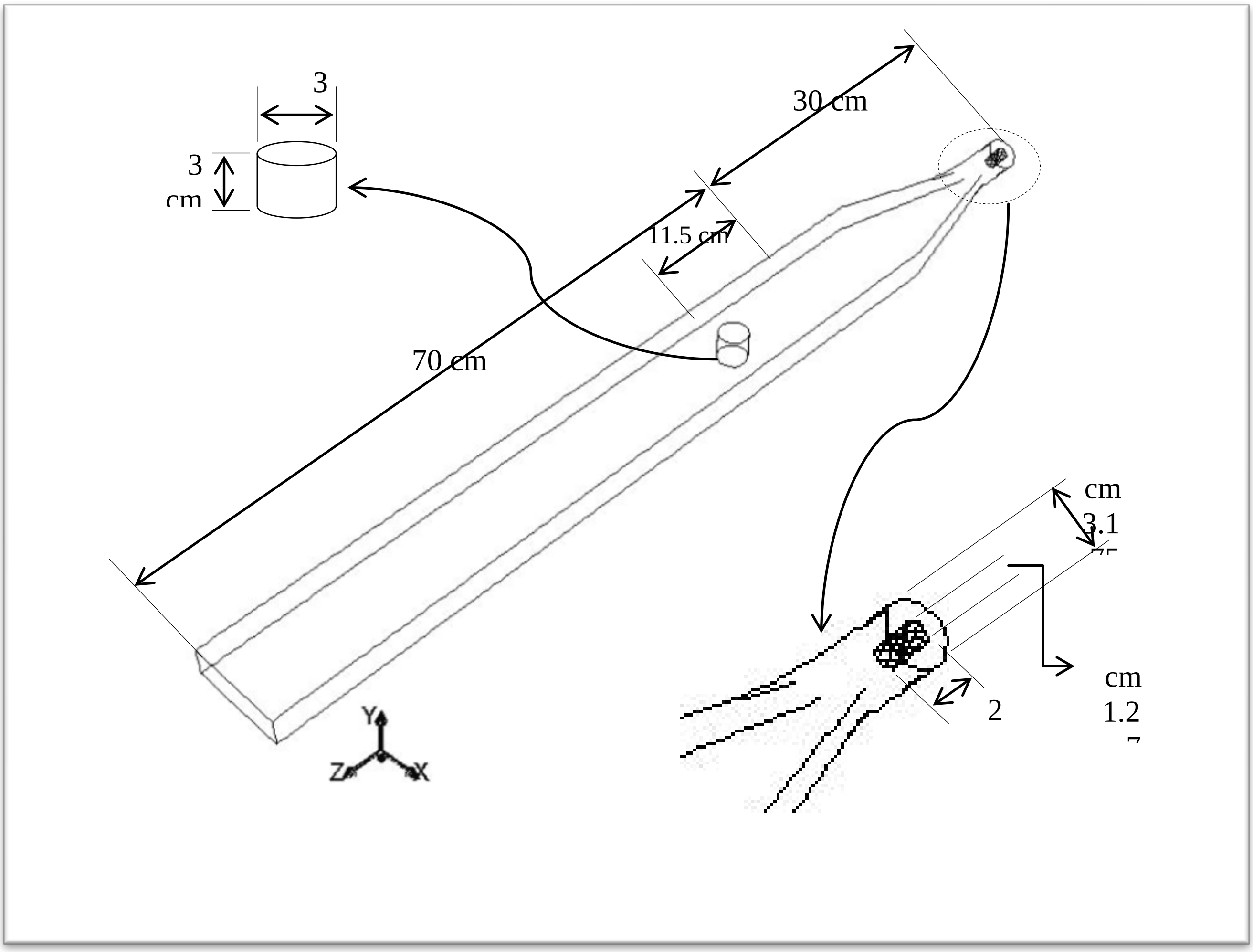

Figure 3 The experimental test section dimensions.

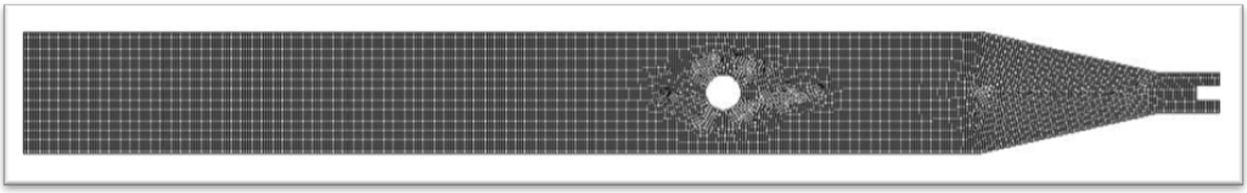

Figure 4 2D model geometry structure mesh.

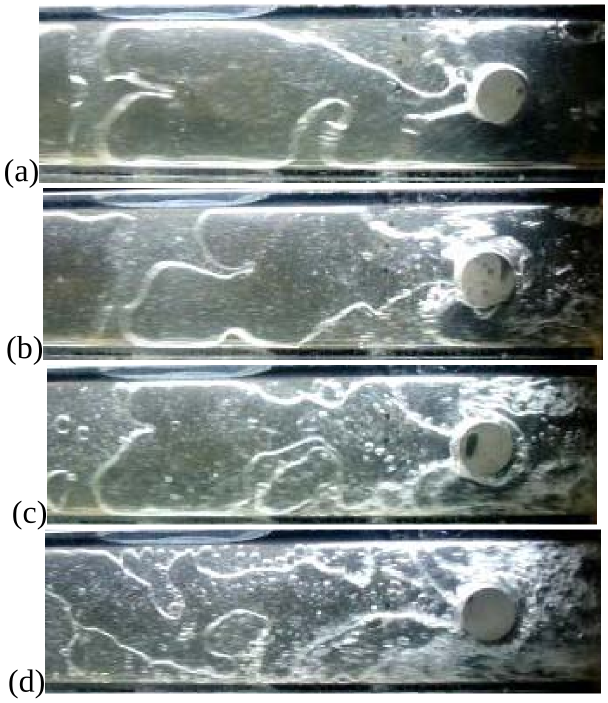

Figure5photographs for the two phase flow behavior for Q_a=10 l/min and Q_w=20, 25, 35 and 45 l/min respectively.

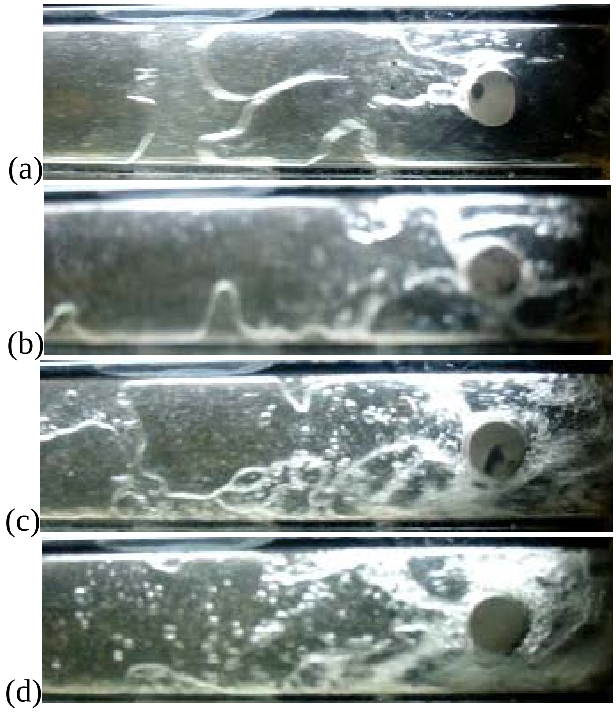

Figure6photographs for the two phase flow behavior for Q_a=20 l/min and Q_w=20, 25, 35 and 45 l/min respectively.

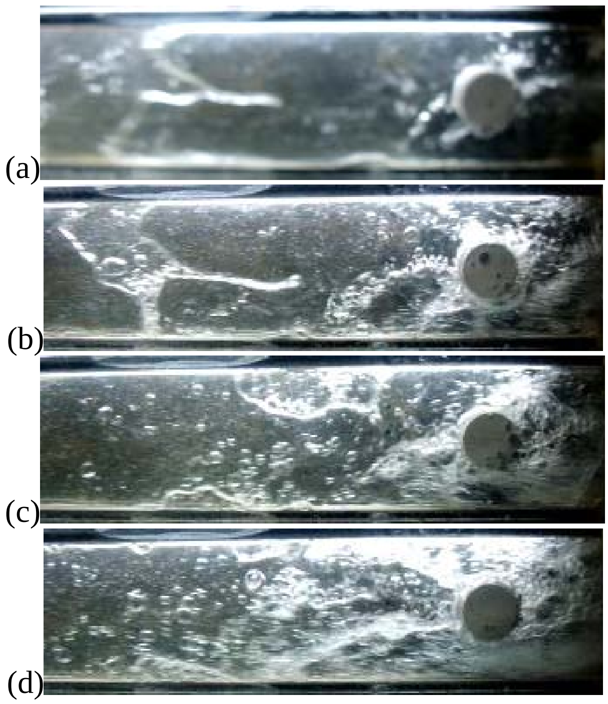

Figure7 photographs for the two phase flow behavior for

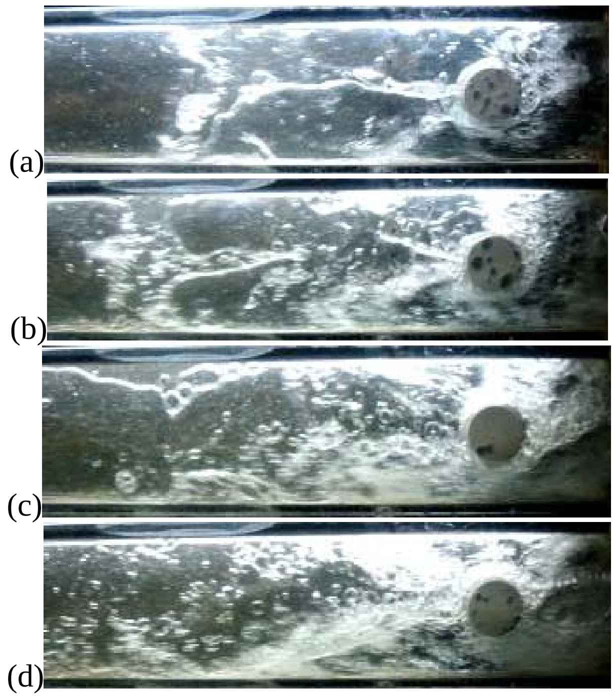

Figure8 photographs for the two phase flow behavior for Q_a=40 l/min and Q_w=20, 25, 35 and 45 l/min

Q_a=30 l/min and Q_w=20, 25, 35 and 45 l/min respectively. respectively.

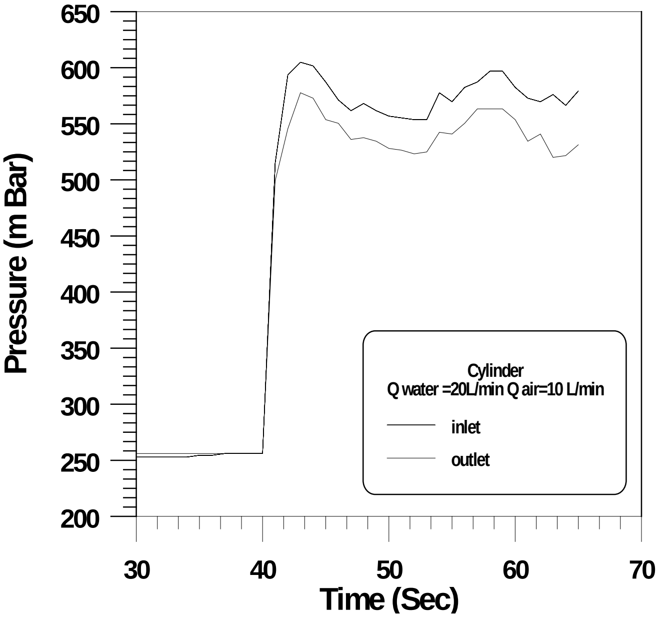

Figure 9 effect of time evolution of pressure for water discharge Q_w=20 l/min and air discharge Q_a=10 l/min.

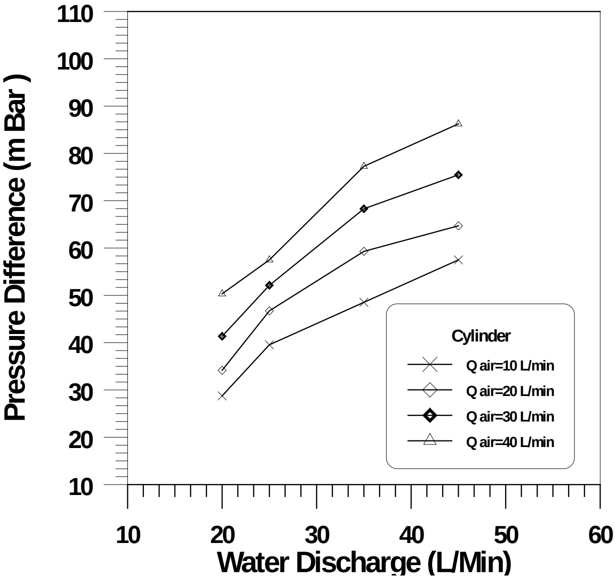

Figure10mean pressure difference with water discharge for different values of air discharge.

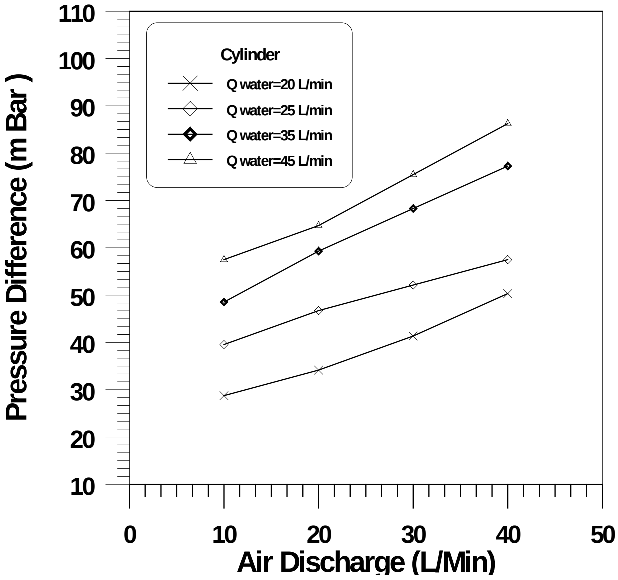

Figure11mean pressure difference with air discharge for different values of water discharge.

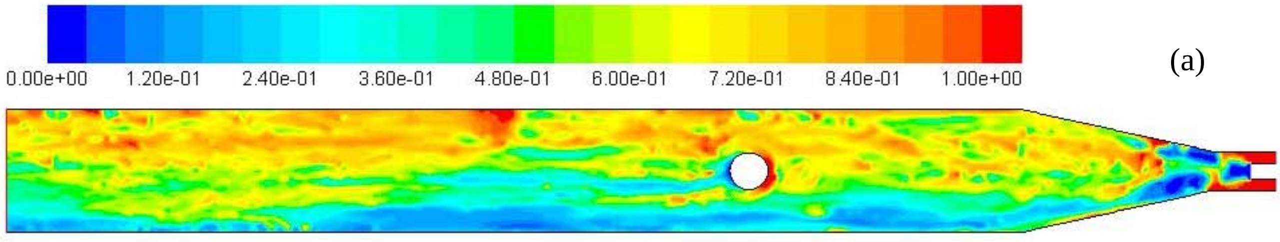

(a)

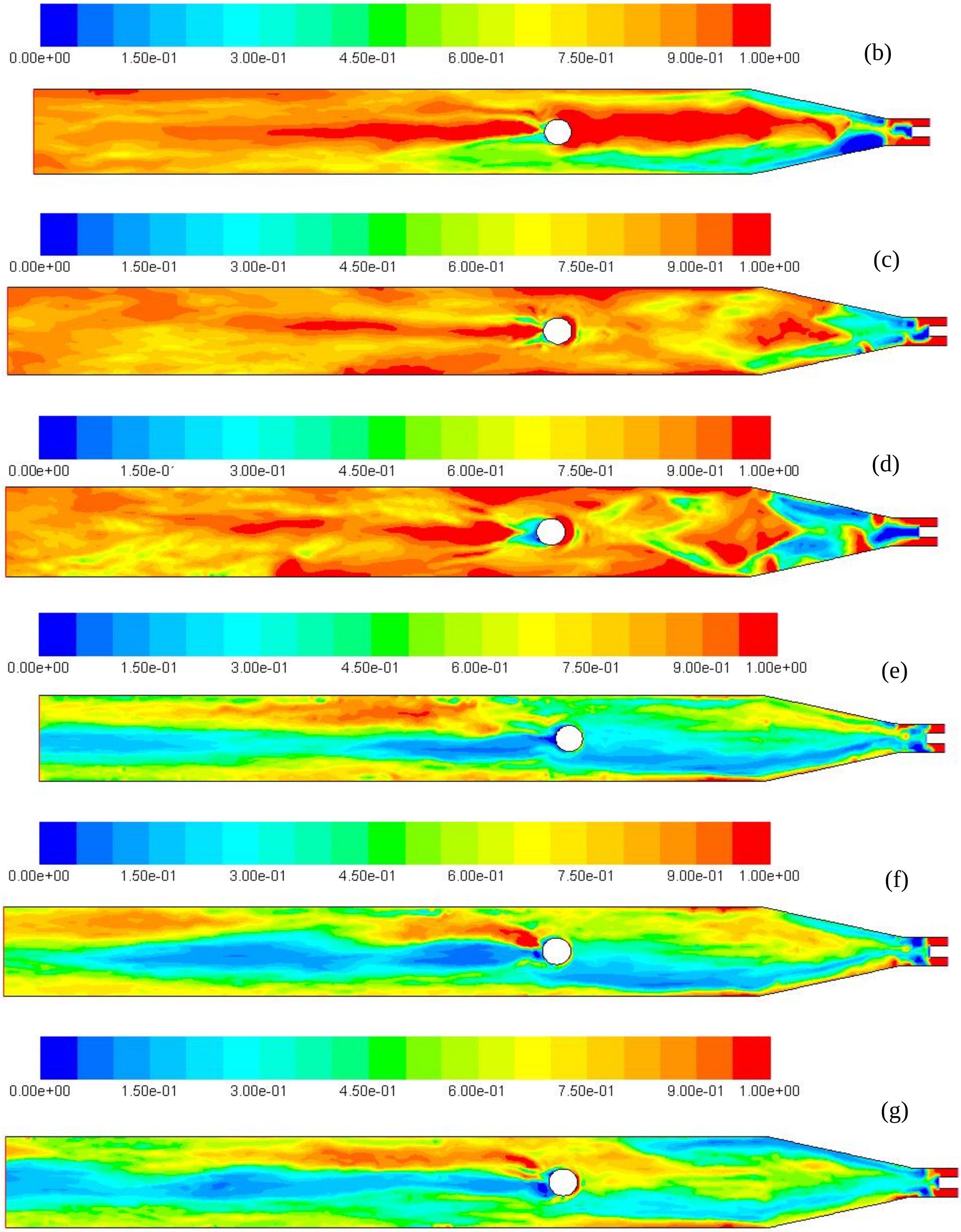

Figure 12volume fraction (water) contours for cases (1, 3, 5, 6, 10, 11 and 12) respectively.

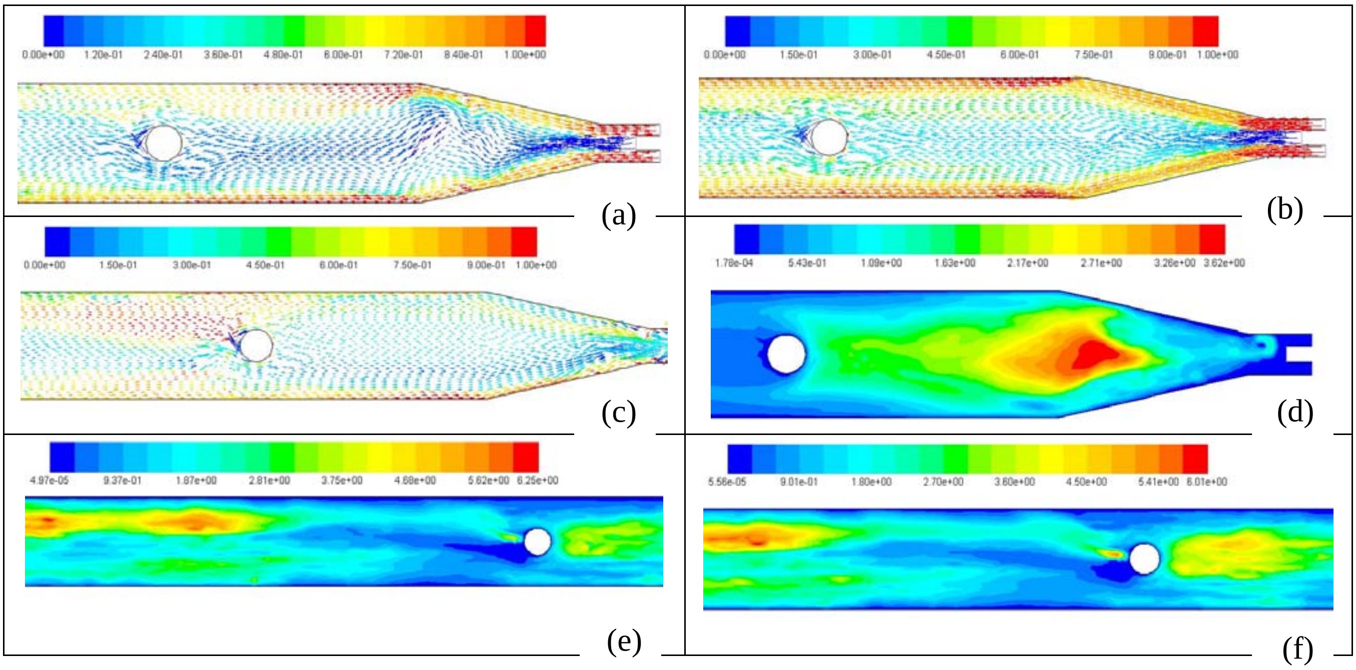

Figure 13velocity vectors colored by volume fraction for cases (2, 4, and 9 respectively) and contours of turbulent viscosity for cases (7, 14 and 16 respectively).

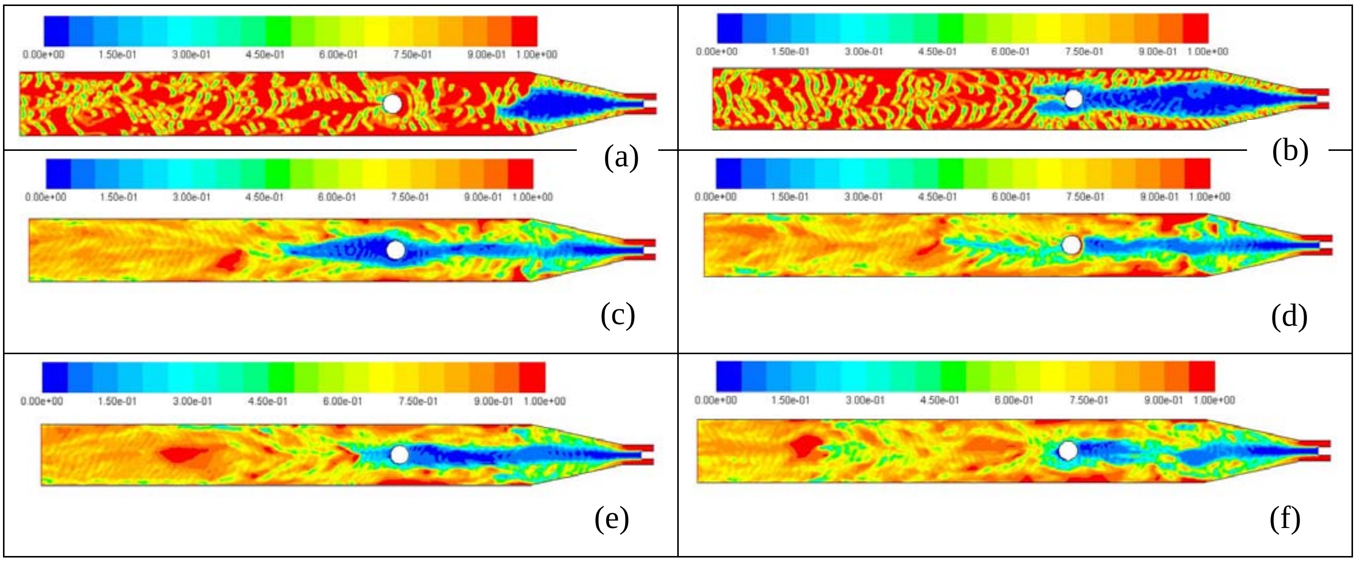

Figure 14volume fraction (water) contours development for unsteady case8.

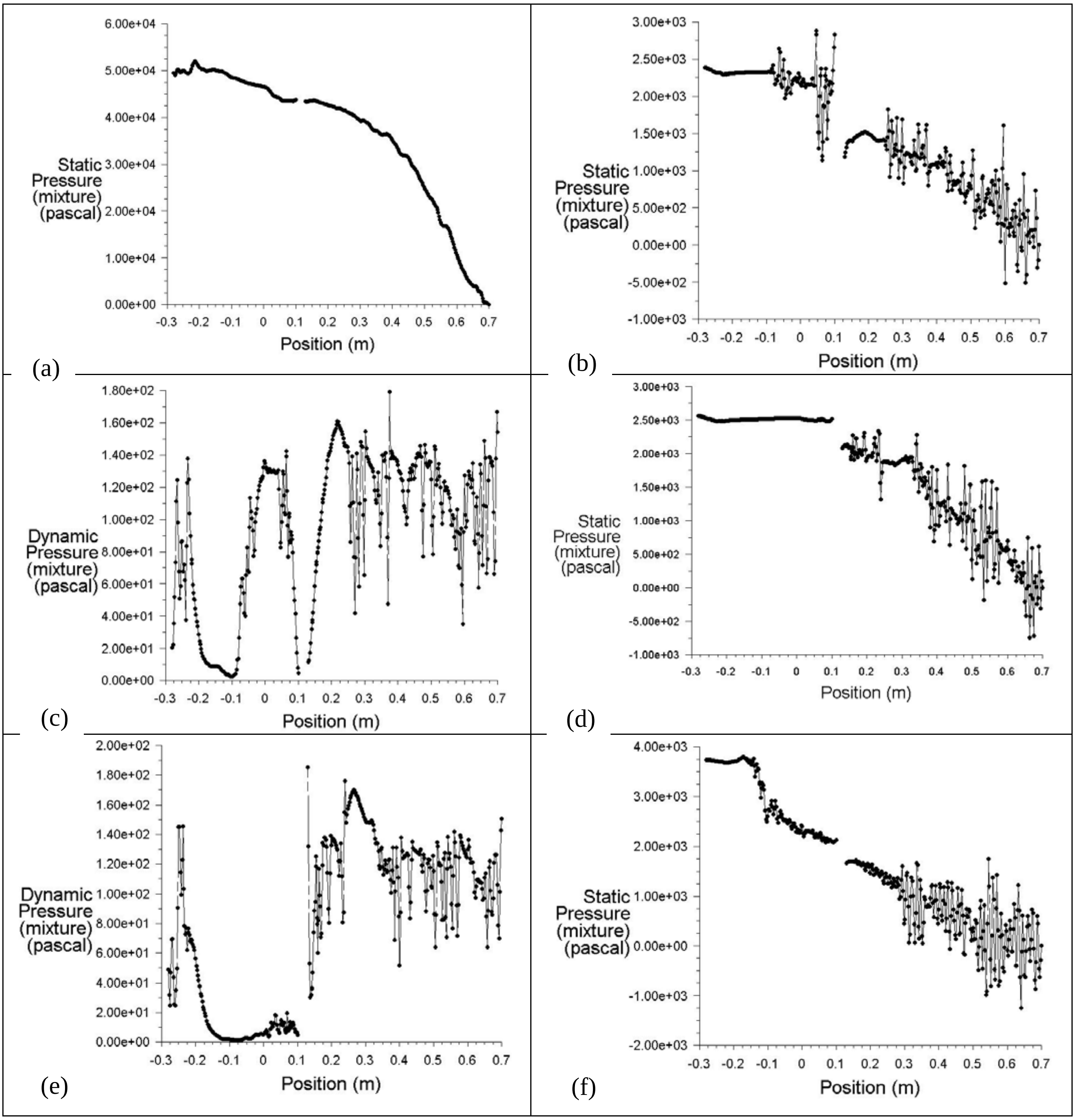
Static Pressure (mixture) (pascal)
Dynamic Pressure (mixture) (pascal)
Position (m)
(a)
(b)
(c)
(d)
(e)
(f)

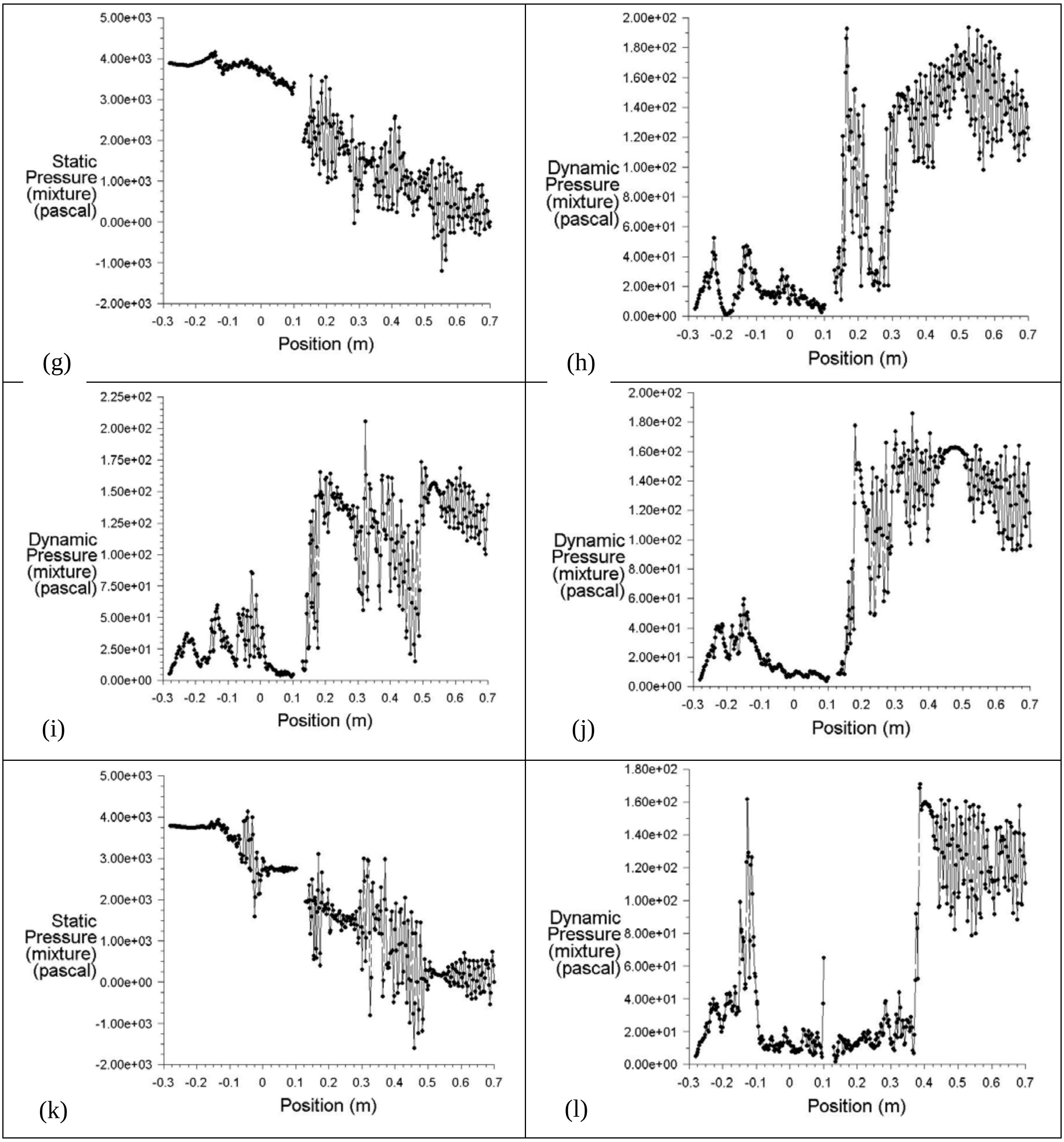

Figure 15static and dynamic pressure distributions of the mixturealong the test rig (1 m) for unsteady case8 at different time steps.

REFERENCES :-

ANSYS 13.0 Help, FLUENT Theory Guide, Mixture Multiphase Model.

Bon Guk Koo, "**Numerical Study of Two -Phase Air-Water Interfacial Flow: Plunging Wave Breaking and Vortex-Interface Interaction**", Ph.D. thesis, University of Iowa, December 2011.

Brennen and Christopher Earls, "**Fundamentals of Multiphase Flow**", Cambridge University Press. ISBN 13 978-0-521-84804-6, 2005.

E. Krepper, P. Ruyer and M. Beyer, D. Lucas, H. M. Prasser, and N . Seiler, "**CFD Simulation of Polydispersed Bubbly Two Phase Flow around an Obstacle**", Hindawi Publishing Corporation, Science and Technology of Nuclear Installations, Volume 2009, Article ID 320738, 12 pages.

Emrah Deniz and Nurdil Eskin, "**Numerical Analysis of Adiabatic Two-Phase Flow through Enlarging Channel**", Istanbul Technical University, Mechanical Engineering Faculty, Istanbul, Turkiye, 2011.

Esam M. Abed and Riyadh S. Al-Turaihi, "**Experimental Study of Two-Phase Flow around Hydrofoil in Open Channel**", Journal for Mechanical and Materials Engineering, Iraq, 2012, accepted and submitted for publication.

Hao Zhou, Guiyuan Mo, Kefa Cen, "**Numerical Investigation of Dispersed Gas–Solid Two-Phase flow Around a Circular Cylinder Using Lattice Boltzmann Method**", Computers & Fluids, vol. 52, pp. 130–138, 2011.

HAORAN MENG, "**On Dispersed Two Phase Flows Past Obstacles**", Ph.D. thesis, Eindhoven University of Technology, ISBN 90-386-04521, 1993.

I. EAMES, J. C. R. HUNT and S. E. BELCHER, "**Inviscid Mean flow through and Around Groups of Bodies**", J. Fluid Mech., vol. 515, pp. 371–389, Cambridge University Press, 2004.

Introductory FLUENT Notes, FLUENT v6.3, Fluent User Services Center, December 2006.

Riyadh S. Al-Turaihi, "**Experimental Investigation of Two-Phase Flow (Gas –Liquid) Around a Straight Hydrofoil in Rectangular Channel**", Journal of Babylon University, Iraq, 2012, accepted and submitted for publication.

V. Talimi, Y. S. Muzychka, S. Kocabiyik, "**A Review on Numerical Studies of Slug flow Hydrodynamics and Heat Transfer in Microtubes and Microchannels**", International Journal of Multiphase Flow, vol. 39, pp. 88–104, 2012.

X. B. Zhang, L. M. Qiu, Y. Gao, X. J. Zhanga, "**Computational Fluid Dynamic Cryogenics**", vol. 48, pp. 432– 438, 2008.